XIX IMEKO World Congress
Fundamental and Applied Metrology
September 6–11, 2009, Lisbon, Portugal

UNCERTAINTY IN THE TEMPERATURE OF SILICON WAFERS MEASURED BY RADIATION THERMOMETRY BASED UPON A POLARIZATION TECHNIQUE

Tohru Iuchi[1], *Atsushi Gogami* [2]

[1] Dept. of Mechanical Engineering, Toyo University, Kawagoe, Japan, iuchi@toyonet.toyo.ac.jp
[2] School of Engineering, Toyo University, Kawagoe, Japan, gn0700130@toyonet.toyo.ac.jp

Abstract – The emissivity behaviour of a silicon wafer under various conditions was theoretically and experimentally investigated. As a result, the quantitative relationship between the ratio of p-polarized radiance to s-polarized one, and polarized emissivities was obtained irrespective of the emissivity change of wafers due to the oxide film thickness under the wide variations of resistivity. Based on the result, we propose a new radiation thermometry method that can measure both the temperature and the spectral polarized emissivity of the silicon wafer, and estimate the uncertainty of the measurements. Currently, the uncertainty of the temperature measurement is estimated to be 3.52 K (2 *k*) and 3.80 (2 *k*) for p-polarization and s-polarization, respectively, in the temperature range over 900 K

Keywords : temperature, emissivity, polarization.

1. INTRODUCTION

The inability to obtain an accurate and reproducible determination of silicon wafer temperature remains a major problem obstructing the achievement of reliable, high-quality processing. Radiometric temperature measurement is crucial in silicon manufacturing processes, because it is a non-contact, contaminant-free method [1-3]. The accuracy of this method is, however, limited by uncertainties in the emissivity of the silicon wafer and of the thin film layers deposited or grown on the wafer surface [4-6]. Therefore, an emissivity compensated method is inevitably required to solve the current difficulties on radiation thermometry [7-8].

In this paper, the emissivity behaviour of a silicon wafer under various conditions is simulated using a simple modelling of the spectral, directional and polarized characteristics of thermal radiation. An excellent relation between polarized radiances and emissivities is derived from the simulated modelling. Successive experiments are carried out, resulting in a practical relationship between the ratio of p-polarized to s-polarized radiances and polarized emissivities that corresponds fairly well with the simulated relation. This findings lead to a new radiation thermometry method that can simultaneously measure both the temperature and the spectral polarized emissivity of the silicon wafer.

In order to accomplish these experiments, a user friendly hybrid surface temperature sensor that the authors have developed is used for the temperature calibration of the silicon wafer [10].

The uncertainty of the proposed radiometric temperature measurement method is analyzed and estimated.

2. EMISSIVITY SIMULATION

Fig. 1 shows a simulation modelling which comprises a bare silicon wafer with an optically smooth surface on which an oxide layer (SiO_2) is grown, where n_1 is the refractive index of air, n_2 and n_3 are the refractive indices of the oxide film and the wafer, respectively.

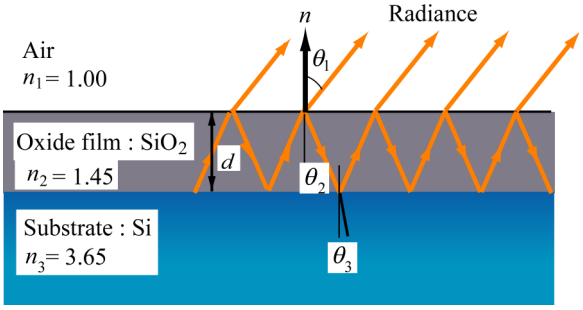

Fig. 1 Simulation model composed of silicon wafer and oxide layer.

The silicon wafer is opaque at a wavelength of λ=0.9 μm because of its band-gap energy of E_g=1.12 eV, thus the radiance from the silicon wafer is limited to the media between the specimen surface and the oxide layer as shown in Fig. 1. Let n_1, n_2 and n_3 be 1.0, 1.45 and 3.65 at λ=0.9 μm [11-12]. Extinction coefficients of both the oxide film and silicon wafer are negligible at λ=0.9 μm near room temperature.

Directional polarized emissivity, $\varepsilon_{p(s)}(\theta_1)$, of the silicon wafer at a direction θ_1 is derived from the following equations [9, 13],

$$\varepsilon_{p(s)}(\theta_1) = 1 - \frac{r_{12p(s)}^2 + r_{23p(s)}^2 + 2r_{12p(s)}r_{23p(s)}\cos\delta}{1 + r_{12p(s)}^2 r_{23p(s)}^2 + 2r_{12p(s)}r_{23p(s)}\cos\delta}, \qquad (1)$$

$$\delta = \frac{2\pi}{\lambda} \cdot 2n_2 \cdot d \cdot \cos\theta_2 , \quad (2)$$

$$r_{12p} = \frac{n_2\cos\theta_1 - n_1\cos\theta_2}{n_2\cos\theta_1 + n_1\cos\theta_2} , \quad (3)$$

$$r_{23p} = \frac{n_3\cos\theta_2 - n_2\cos\theta_3}{n_3\cos\theta_2 + n_2\cos\theta_3} , \quad (4)$$

$$r_{12s} = \frac{n_1\cos\theta_1 - n_2\cos\theta_2}{n_1\cos\theta_1 + n_2\cos\theta_2} , \quad (5)$$

$$r_{23s} = \frac{n_2\cos\theta_2 - n_3\cos\theta_3}{n_2\cos\theta_2 + n_3\cos\theta_3} , \quad (6)$$

$$n_1\sin\theta_1 = n_2\sin\theta_2 = n_3\sin\theta_3 , \quad (7)$$

where δ is the phase delay of an electromagnetic wave inside the oxide film. $r_{12p(s)}$ and $r_{23p(s)}$ are amplitudes of the reflection of p- (or s-) polarized waves at the interface between air and the oxide film, and the oxide film and the silicon wafer substrate, respectively.

The p-polarized and s-polarized radiances, $L_p(T)$ and $L_s(T)$, at a direction θ_1 that are emitted by the silicon wafer at a temperature, T, are described, respectively, as

$$L_p(T) = \varepsilon_p(\theta_1) \cdot L_{\lambda,b}(T) , \quad (8)$$

$$L_s(T) = \varepsilon_s(\theta_1) \cdot L_{\lambda,b}(T) , \quad (9)$$

And the polarized emissivity, $\varepsilon_{p(s)}(\theta_1)$, is defined as Eq. (10),

$$\varepsilon_{p(s)}(\theta_1) = \frac{L_{p(s)}(T)}{L_{\lambda,b}(T)} , \quad (10)$$

where $L_{\lambda,b}(T)$ is the spectral blackbody radiance at T and λ.

Let R_{ps} be the ratio of p-polarized to s-polarized radiances. Then, R_{ps} is expressed as

$$R_{ps} = \frac{L_p(T)}{L_s(T)} = \frac{\varepsilon_p(\theta_1)}{\varepsilon_s(\theta_1)} . \quad (11)$$

Fig. 2 shows simulated results of directional polarized emissivity, $\varepsilon_{p(s)}(\theta_1)$, of a bare silicon wafer at λ=0.9 μm.

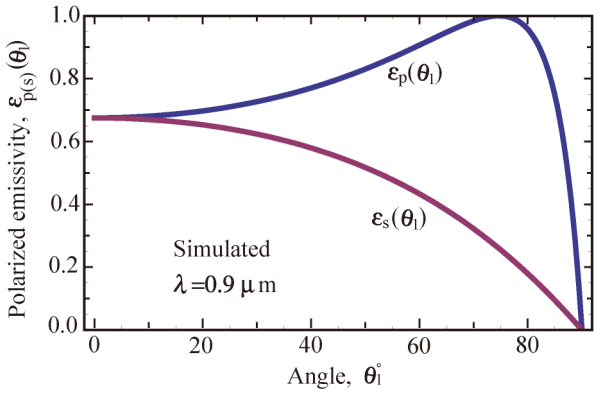

Fig. 2 Simulated results of directional polarized emissivity of a bare silicon wafer at λ=0.9 μm.

Fig. 3 shows simulated relationships between the ratio of polarized radiances, R_{ps}, and polarized emissivity, $\varepsilon_{p(s)}(\theta_1)$ at θ_1=70° and λ=0.9 μm, where oxide film thickness, d, ranges between 0 (bare) and 950 nm. It is apparent from Fig. 3 that once the ratio, R_{ps}, is determined from the measurements of $L_p(T)$ and $L_s(T)$, then the p-polarized emissivity, $\varepsilon_p(\theta_1)$, or s-polarized emissivity, $\varepsilon_s(\theta_1)$, of the silicon wafer can be uniquely obtained irrespective of emissivity variations caused by the change of oxide film thickness. This finding leads to new radiation thermometry of silicon wafers based upon a polarization technique.

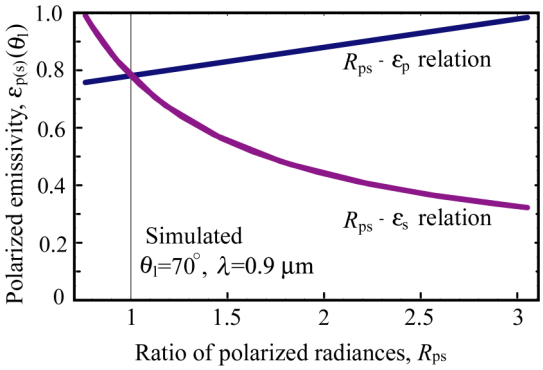

Fig. 3 Simulated relationships between R_{ps} and $\varepsilon_{p(s)}(\theta_1)$ at θ_1=70° and λ=0.9 μm.

3. EXPERIMENTAL APPARATUSES

In order to confirm the simulated results, some experiments were achieved. Table 1 shows measurement conditions including silicon wafers prepared for experiments. Resistivity, ρ, and oxide layer thickness, d, of specimens are covered with wide ranges from 0.01 to 2000 Ωcm and from 30 to 950 nm, respectively. Resistivity is deeply related to the impurity concentration of a silicon wafer. Table 2 shows a relation between the impurity concentration and resistivity of silicon wafers [14].

Table 1 Measurement conditions for experiments.

Specimen n-type silicon wafer, (100) plane Dimension: 0.75 mm thick and 76.2 mm diameter (3 in.) Resistivity: ρ = 0.01, 1 and 2000 Ωcm Oxide film (SiO_2) thickness: d=30, 150, 350, 550, 750 and 950 nm. Surface roughness: R_a = 0.03 μm (specular)
Temperature T = 900 to 1000 K
Wavelength λ = 0.9 μm

Table 2 Relation between impurity concentration and resistivity of silicon wafers at room temperature.

Resistivity, Ωcm	Impurity concentration, cm^{-3}
0.01	~8 x 10^{19}
1	~6 x 10^{15}
2000	~3 x 10^{14}

Fig. 4 shows the experimental apparatus for the measurement of directional polarized emissivity of silicon wafers. The radiance emitted from the area of 2 mm in

diameter of the specimen surface is divided into p- and s-polarized radiances by the polarizing beam-splitter cube (05FC 16 PB.7, Newport) and transmitted through optical fibers, and is finally detected by the polarized radiometer (IR-FBWS-SP, Chino) sensitive at a wavelength of 0.9 μm [9]. The directional polarized emissivity, $\varepsilon_{p(s)}(\theta_l)$, that is the ratio of the specimen radiance to the blackbody one at the same temperature, is continuously measured at angle, θ_l, between 0° and 85° in accordance with the rotation of the supporting bar.

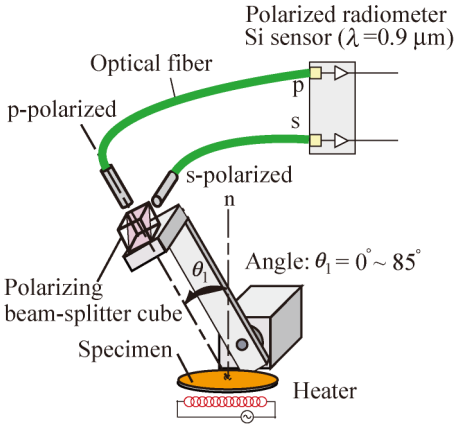

Fig. 4 Measurement apparatus of directional polarized emissivity.

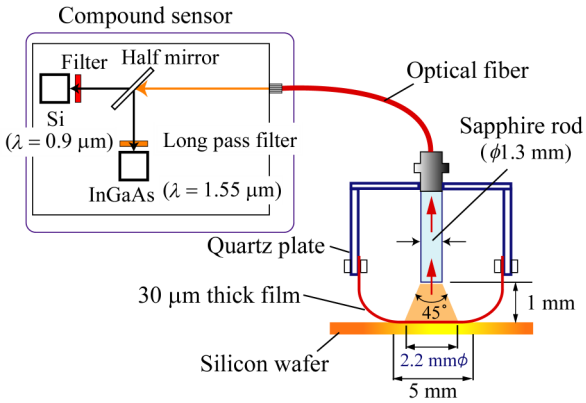

Fig. 5 Hybrid surface temperature sensor developed for the temperature calibration of silicon wafers.

Fig. 5 shows a schematic diagram of a newly developed hybrid surface temperature sensor [10]. The tip of this sensor includes a rectangular thin film of super alloy, Hastelloy (thickness: 30 μm, width: 5mm, length: 17 mm) and a sapphire rod (diameter:1.3 mm). Both ends of the thin metal film are supported by quartz plates, and its central portion of 5 mm in length instantaneously contacts the surface of a silicon wafer. The thin film and the sapphire rod are spaced closely with the gap of 1 mm. The radiant flux from the area (diameter: 2.2 mm) of the rear surface of the thin film is incident on the sapphire rod and is transmitted through an optical fiber. The radiant flux is then detected as radiance signals by a compound sensor comprised of Si and InGaAs detectors with sensitivities at 0.9 μm and 1.55 μm, respectively. When the emissivity of the rear surface of the film is known, the temperature of the film can be derived from the radiance signal. At this time, the surface temperature of the silicon wafer is accurately determined. The response time of this sensor is within 1s. The temperature range is 600 K to 1,000 K at the moment. The principle of this sensor is based on the assumption that the temperature of the thin film is spatially uniform at any instant during the transient process [10, 15].

Fig. 6 is an experimental system for the study of the emissivity behaviour of silicon wafers composed of the polarized radiometer that measures directional polarized emissivities (in Fig. 4) and the hybrid surface temperature sensor that measures surface temperatures of silicon wafers (in Fig. 5). A silicon wafer is put onto the heating furnace and controlled at a high temperature between 900 K and 1,000 K by the temperature controller (KP1000, Chino). The surface temperature, T, of the silicon wafer is monitored by the hybrid surface temperature sensor, and p- and s-polarized radiances, $L_p(T)$ and $L_s(T)$ are simultaneously measured by the polarized radiometer. The directional polarized emissivity, $\varepsilon_{p(s)}(\theta_l)$, and the ratio, R_{ps}, in Eqs. (10) and (11) are calculated using these signals, respectively.

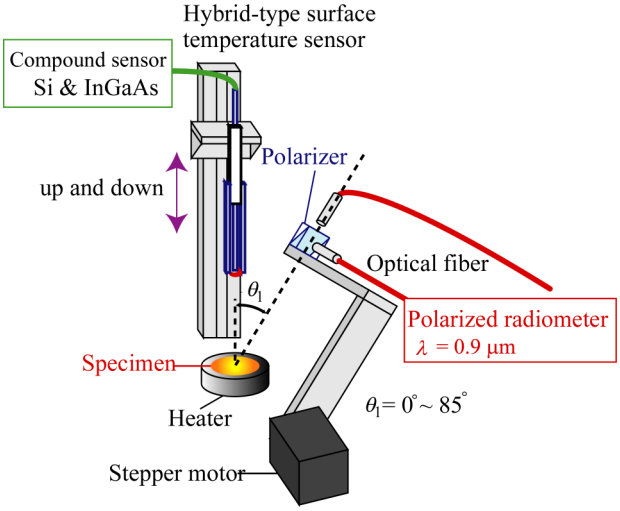

Fig. 6 Experimental system for the polarized emissivity measurement composed of the polarized radiometer and the hybrid surface temperature sensor.

4. EXPERIMENTAL RESULTS

We have prepared many silicon wafers with different resistivity and oxide film thickness as shown in Table 1 to study the reproducibility of the emissivity behaviours that were represented by the simulated results in Figs. 2 and 3.

Fig. 7 shows experimental results of directional polarized emissivity, $\varepsilon_{p(s)}(\theta_l)$, of a bare silicon wafer (d=0 nm) with resistivity of ρ=1 Ωcm at T=1000 K and λ=0.9 μm. In the figure, the simulated result is also shown with dotted line. It is clearly observed that the experimental result corresponds well to the simulated one except angles over θ_l=85 ° because of the technical limitation of an angle measurement.

Fig. 8 compares simulated relationships between oxide film thickness, d, and polarized emissivitity, $\varepsilon_{p(s)}(\theta_l)$, with experimental ones at a temperature of T=1,000 K, a direction of θ_l=30° and a wavelength of λ=0.9 μm. Both p- and s-polarized emissivities in the simulated results are observed to change periodically with increasing film thickness. The experimental results, though these are several points, also show similar behaviours as the simulated ones.

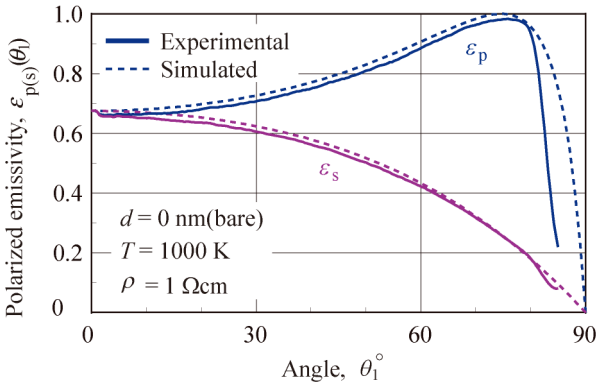

Fig. 7 Experimental and simulated results of directional polarized emissivities, $\varepsilon_{p(s)}(\theta_l)$, of a bare silicon wafer (d= 0 nm).

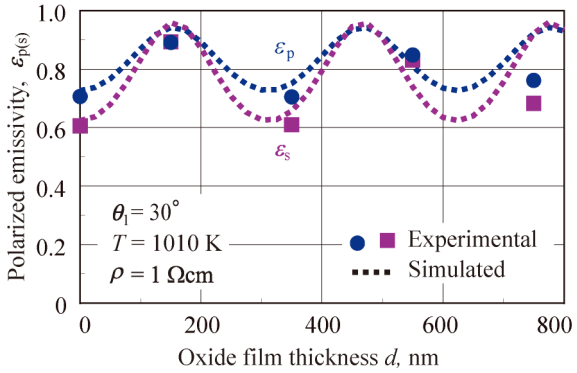

Fig. 8 Experimental and simulated relationships between oxide film thickness, d, and polarized emissivity, $\varepsilon_{p(s)}(\theta_l$=30°), of silicon wafers.

Fig. 9 shows another measurement example of the directional polarized emissivities of silicon wafers with different oxide film layers, d=30 nm and 150 nm. It is seen that both p- and s-polarized emissivities ($\varepsilon_p(\theta_l)$ and $\varepsilon_s(\theta_l)$) drastically change with the oxide film thickness. These emissivity variations result in quite large temperature errors in the conventional radiation thermometry.

Fig. 10 displays experimental results of directional polarized emissivities, $\varepsilon_{p(s)}(\theta_l)$, of silicon wafers with different resistivity, ρ, from 0.01 to 2000 Ωcm, different temperature, T, from 900 to 1,000 K. The oxide film thickness, d, grown on the wafers is 30 nm. All data of both p-polarized and s-polarized emissivities are overlapped within some fluctuations in the figure. It is clearly observed from the results that both p-polarized and s-polarized emissivities largely change with the angle, θ_l, but the effect of resistivity, ρ, and the temperature, T, on the emissivity are little. Similar experiments have been carried out for silicon wafers with different oxide films that cover from 30 to 950 nm thick. The directional polarized emissivity behaves as in Fig. 10 under the same oxide film thickness, though it shows a different pattern when a thickness, d, is different. Uncertainty of the reproducibility of emissivity behaviour is analyzed in the section 4.

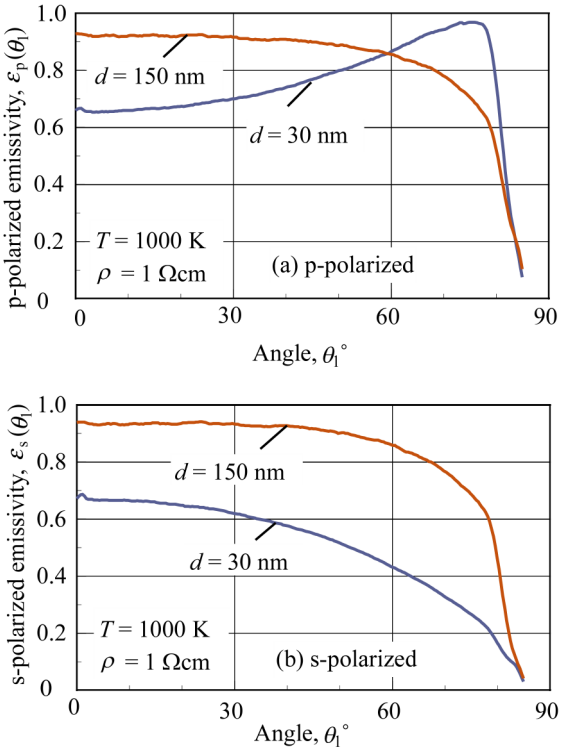

Fig. 9 Experimental results of directional polarized emissivities, $\varepsilon_{p(s)}(\theta_l)$, of silicon wafers with different oxide film thickness (d=30 and 150 nm).

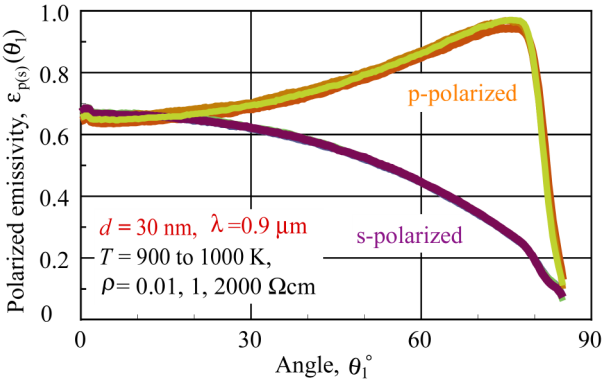

Fig. 10 Experimental results of directional polarized emissivity, $\varepsilon_{p(s)}(\theta_l)$, of silicon wafer of d=30 nm with different resistivity, ρ, and temperature, T.

Based on the above experimental results, we considered an emissivity-compensated radiation thermometry method. Fig. 11 shows the experimental and simulated relationships between R_{ps}, the ratio of the polarized radiance,

and polarized emissivity, $\varepsilon_{p(s)}(\theta_l)$, of silicon wafers at an angle θ_l of 70º. Solid lines show the simulated relations, and the circles and the square points are experimental data. This relations are valid for wide range of resistivity between 0.01 to 2000 Ωcm, the oxide film thickness from bare (d=0 nm) to 950 nm, and the temperature from 900 to 1,000 K. These results confirm that there is one-to-one relation between the ratio, R_{ps}, and p-polarized or s-polarized emissivities irrespective of wide variations of emissivity of silicon wafers. This means that once the polarized radiances, L_p(T) and L_s(T), are measured and its ratio, R_{ps}, is calculated, p-polarized emissivity, $\varepsilon_p(\theta_l)$, or s-polarized one, $\varepsilon_s(\theta_l)$, at an angle, θ_l, can uniquely be determined, resulting in an accurate temperature measurement.

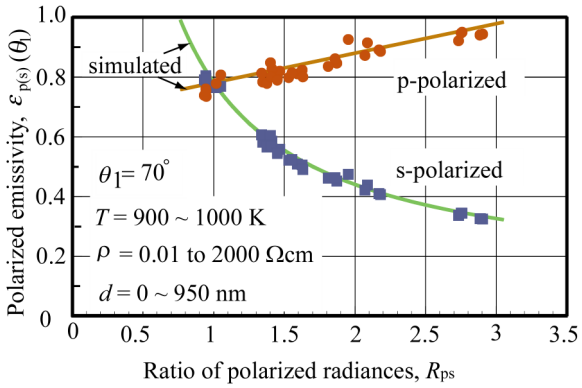

Fig. 11 Experimental and simulated relations between R_{ps} and $\varepsilon_{p(s)}(\theta_l)$ of silicon wafers with wide range of resistivity and oxide film thickness at θ_l=70º and λ=0.9 μm.

4. UNCERTAINTY OF MEASUREMENTS

Primary factors involved in uncertainties of the measurements are (a) hybrid surface temperature sensor to monitor the surface temperature of a specimen and (b) the measurement principle including a polarized radiometer.

4.1. Hybrid surface temperature sensor

The uncertainty of (a) a hybrid surface temperature sensor has been analysed in detail in a separate paper [16]. Uncertainty sources are fluctuation of the hybrid sensor, radiometer output repeatability, fluctuation of the silicon wafer surface, emissivity variation of the pseudo-blackbody coatings and fluctuation of the temperature distribution of a specimen surface. Overall uncertainty, u_h, caused by the hybrid surface temperature sensor is estimated to be 1.06 K.

4.2. Experimental relation of measurement principle

The uncertainty sources of (b) the measurement principle are mainly divided into two parts; (i) the polarized radiometer that detects p- and s-polarized radiances of silicon wafers and (ii) the deviation from the experimental relationship between the ratio of polarized radiances, R_{ps} and polarized emissivity, $\varepsilon_{p(s)}(\theta_l)$.

(i) uncertainty of the polarized radiometer in Fig. 4 is composed of the output repeatability, u_r, that is given by the manufacturer (Chino) and temperature fluctuation, u_a, in air. u_r is specified as 0.70 K at 1,000 K and the u_a is measured to be 0.24 K at 1,000 K.

(ii) uncertainty of the experimental relationship of the measurement principle is caused by the deviation, u_r, from the R_{ps}-$\varepsilon_{p(s)}(\theta_l)$ relation.

The experimental relationships between R_{ps} and $\varepsilon_{p(s)}(\theta_l)$ in Fig. 11 are expressed as shown in Eqs. (12) and (13) for p- and s-polarizations, respectively, using the method of least squares,

For p-polarization,

$$\varepsilon_p(\theta_l) = 0.1019 \times R_{ps} + 0.6572, \tag{12}$$

and for s-polarization,

$$\varepsilon_s(\theta_l) = -0.0892 \times R_{ps}^3 + 0.6358 \times R_{ps}^2 - 1.6126 \times R_{ps} + 1.8281. \tag{13}$$

The standard deviations of measured emissivities, σ_p, and σ_s, for p- and s-polarizations are 0.016 and 0.010, respectively. The standard deviations of converted temperatures, u_p and u_s, originated from the deviations of the emissivities, σ_p and σ_s, are calculated using the following equations [17],

$$u_{p(s)} = \frac{1}{n} \cdot \frac{\sigma_{p(s)}}{\varepsilon_{p(s)}} \cdot T, \tag{14}$$

$$n = \frac{14388}{\lambda \cdot T}, \tag{15}$$

where the representative values of polarized emissivities, ε_p and ε_s, are 0.85 and 0.45, respectively, that are measured at 900 K to 1000 K and λ=0.9 μm are taken as $\varepsilon_{p(s)}$ to calculate $u_{p(s)}$.

u_p and u_s are calculated as 1.18 K and 1.39 K at T=1,000 K, respectively.

4.3. Other factors

All measurement signals including the polarized radiances of the radiometer and the hybrid surface temperature sensor are transformed and processed by an A/D converter (Model NR-1000, Keyence) to obtain digital quantities having a resolution of 16 bits and a sampling rate of 100 ms. The uncertainties of all digitized signals are neglected, because the resolution is less than 0.1 K at reduced temperature.

4.4. Overall uncertainty

Overall standard uncertainty, $u_{overall}$, is calculated from the following Eq. (16),

$$u_{overall} = \sqrt{u_h^2 + u_r^2 + u_a^2 + u_{p(s)}^2}. \tag{16}$$

The overall uncertainty of the radiation thermometry based on a polarized technique is shown in Table 3. The expanded uncertainty, $u_{expanded}$, (k=2) of the measurement principle is 3.52 K for p-polarization, and 3.80 K for s-polarization, respectively at the moment.

The uncertainty of this radiation thermometry will be much reduced when the improvements of the hybrid surface temperature sensor and the polarized radiometer are performed.

Table 3 Uncertainty budget for the radiation thermometry based upon the polarized technique at T=1,000 K.

Uncertainty source		u_i / K
(a) Hybrid surface temperature sensor		u_h=1.06
(b) Measurement principle		
(i) Polarized radiometer output		u_r=0.70
Temperature fluctuation in air		u_a=0.24
(ii) Experimental relation of measurement principle		
Deviation of polarized emissivity		
		u_p=1.18
		u_s=1.39
$u_{overall}$	p-polarization	1.76
	s-polarization	1.90
$u_{expanded}$ (k=2)	p-polarization	3.52
	s-polarization	3.80

5. CONCLUSIONS

Emissivity behaviour of silicon wafers was comprehensively investigated from both simulated and experimental aspects.

Some concluding remarks are summarized as follows,

1. Polarized emissivity of silicon wafers largely and cyclically changes with the oxide film thickness, d.
2. Experimental results of polarized emissivities of silicon wafers that cover wide range of resistivity, ρ, from 0.01 to 2000 Ωcm correspond well with simulated ones at high temperatures over T=900 K and a wavelength of λ=0.9 μm. This means that resistivity closely relevant to impurity concentration do not affect the emissivity of silicon wafers over 900 K.
3. The emissivity-compensated radiation thermometry using the relationship between R_{ps} that is the ratio of polarized radiances and polarized emissivity, $\varepsilon_{p(s)}(\theta_1)$, is very promising. Currently, the overall uncertainty (k=2) of the method is estimated to be 3.52 K for p-polarization use, and 3.80 K for s-polarization use, respectively, in the temperature range over 900 K, irrespective of large emissivity variations and wide change of resistivity.
4. The hybrid surface temperature sensor is proved to be a powerful device to calibrate the surface temperature of silicon wafers.

ACKNOWLEDGMENTS

The authors would like to thank K. Hiraka at Chino Corp. for his contribution to this study when he was a graduate student at Toyo Unversity.

The present research was supported in part by the Ministry of Education, Science, Sports and Culture through a Grand-in-Aid for Scientific Research (C) (Project Number 20560403) and as a "High-Tech Research Center" Project for Private Universities through matching funds from the Ministry of Education, Sports, Science, and Technology, 2004-2008.

REFERENCES

[1] F. Roozeboom and N. Parekh, "Rapid thermal processing systems", J. Vacuum Science Technology, vol. B8, nº. 6, pp. 1249-1259. 1990.

[2] R. L. Anderson, "Review of temperature measurements in the semiconductor industry", *TEMPERATURE, Its Measurement and Control in Science and Industry*, Edited by J. Schooley, New York, AIP, vol. 6, pp. 1117-1122, 1992.

[3] B. E. Adams, "The challenges of temperature measurement in the semiconductor industry", *7th International Symposium on Temperature and Thermal Measurements in Industry and Science*, edited by J. F. Dubbeldam and M. J. de Groot, NMi, Delft, pp. 1-10, 1999.

[4] T. Sato, "Spectral emissivity of silicon", *J. J. Appl. Phys.*, vol. 6, nº. 3, pp. 339-347, 1967.

[5] P. J. Timans, "Emissivity of silicon at elevated temperatures", *J. Appl. Phys*., vol. 74, nº.10, pp. 6353-6364, 1993.

[6] D. H. Chen, D. P. DeWitt, B, K. Tsai, K. G. Kreider and W. A. Kimes, "Effects of wafer emissivity on rapid thermal processing temperature measurement", *TEMPERATURE, Its Measurement and Control in Science and Industry*, Edited by D. C. Ripple, New York, AIP, vol. 7, pp. 735-740, 2003.

[7] B. Adams, A. Hunter and A. Rubinchik, "A novel integrated pyrometer-emissometer which enables accurate temperature measurements of suface with unknown emissivities", 8th *International Symposium on Temperature and Thermal Measurements in Industry and Science*, edited by B. Fellmuth, J. Seidel and G. Scholz, VDE Verlag GMBH, Berlin, pp. 975-980, 2001.

[8] T. Iuchi, "In-situ temperature measurement of silicon wafers (translated into English)", T*rans. SICE*, vol. 47, nº. 5, pp. 395-402, 2008.

[9] T. Iuchi and A. Gogami, "Emissivity compensated radiation thermometry of silicon wafers during the growth of oxide films", *TEMPBEIJING 2008*, pp. 4A1-4A7, Beijing, China, October, 2008.

[10] K. Hiraka, R. Shinagawa, A. Gogami and T. Iuchi, "Rapid response hybrid-type surface temperature sensor", *Int. J. Thermophysics*, vol. 29, nº. 2, pp. 1166-1173, 2008.

[11] H. R. Philip, *Silicon Dioxide (SiO_2), Handbook of Optical Constants of Solid*, Edited by E. D. Palik, Academic Press, New York, pp. 719-763, 1985.

[12] D. F. Edwards, *Silicon (Si), Handbook of Optical Constants of Solid*, Edited by E. D. Palik, Academic Press, New York, pp. 547-569, 1985.

[13] M. Born and E. Wolf, *Principles of Optics*, 7th edition, Cambridge Univ. Press, Cambridge, pp. 735-758, 1999.

[14] S. M. Sze, *Semiconductor Devices, Physics and Technology*, 2nd ed., Wiley, New York, pp. 51-56, 2002.

[15] F. P. Incropera and D. P. DeWitt, *Fundamentals of Heat and Mass Transfer*, Wiley, New York, pp. 240-254, 1988.

[16] T. Iuchi and A. Gogami, "Uncertainty of a hybrid surface temperature sensor for silicon wafers and its comparison with an embedded thermocouple", Rev. Sci. Instr., submitted.

[17] G. D. Nutter, *Radiation Thermometry-The Measurement Problem*, *Applications of Radiation Thermometry,* Edited by D. P. DeWitt and J. C. Richmond, ASTM, Philadelphia, pp. 3-23, 1986.